Electronic Supporting Information

Synthesis and Solution Properties of Telechelic Poly(2-isopropyl-2-oxazoline) Bearing Perfluoro End Groups

Na Xue, [a] Xiaoming Hou, [b] Xing-Ping Qiu, [c] Xiaotao Song, [b] Qingguo Feng, *[b] and Xiaozhi Liu *[a]

[a]Tianjin Key Laboratory of Epigenetics for Organ Development of Preterm Infants, Central Laboratory, Tianjin Fifth Central Hospital, Tianjin 300450, China

[b]Department of Critical Care Medicine, Tianjin Fifth Central Hospital, Tianjin 300450, China

[c]Department of Chemistry, University of Montreal, CP6128 Succursale Centre Ville, Montreal QC Canada H3C 3J7

*Corresponding author: lxz7997@126.com, anginagi@163.com

Polymerization kinetics: ^{1}H NMR spectroscopy was used to track the kinetics of the polymerization based on the changes in signal strength due to the resonances of the methylene protons of the monomer and the polymer. Fig. S1 presents a slightly upward curvature of ln([M_0]/[M_t]) plot as a function of polymerization time, indicating that initiation was slower than chain propagation.[30] The ln([M_0]/[M_t]) vs time relationship is virtually linear in the late stages of the polymerization, showing that the concentrations of propagating species remained constant and termination reactions were absent in the system. In addition, for a given conversion, the polymerization degree (DP) of the polymer was in good agreement with the initial feed ratio of monomer/initiator, which supports our assumption that all the initiator was consumed in the late stages of the polymerization. Table S1 presents details of the polymerization and molecular weight characterizations of N_3PIPOZ.

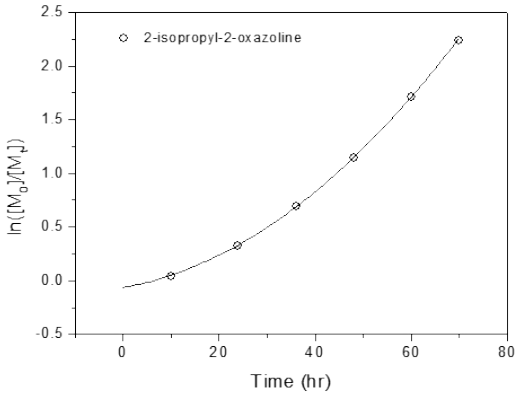

Fig. S1 Kinetic plot of N_3IPOZ polymerization initiated by diethylene glycol di(p-toluenesulfonate) in acetonitrile at 65 °C.

Table S1 Polymerization and molecular weight characterizations of N_3PIPOZ

polymer	Time (hour)	Yield (%)	M_n (kDa)	DP	M_w/M_n
N_3PIPOZ	72	88	7.6	68	1.12

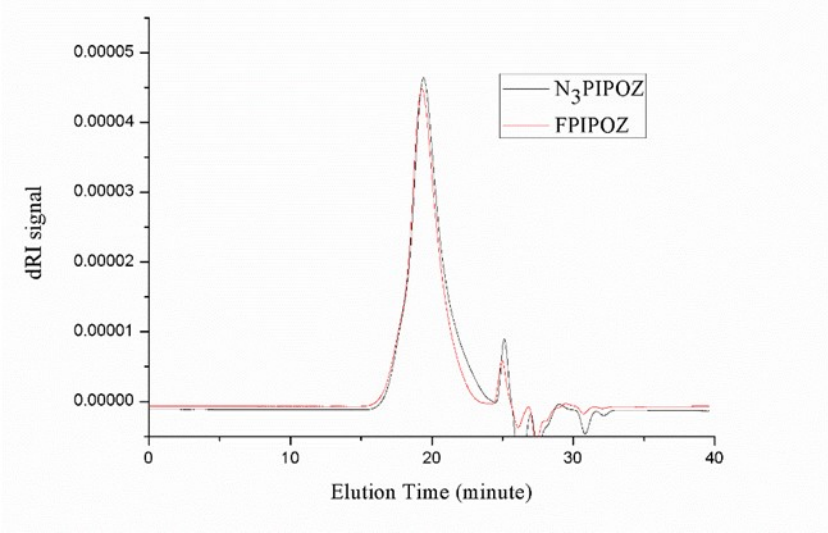

Fig. S2 GPC traces of N_3PIPOZ and FPIPOZ in DMF.

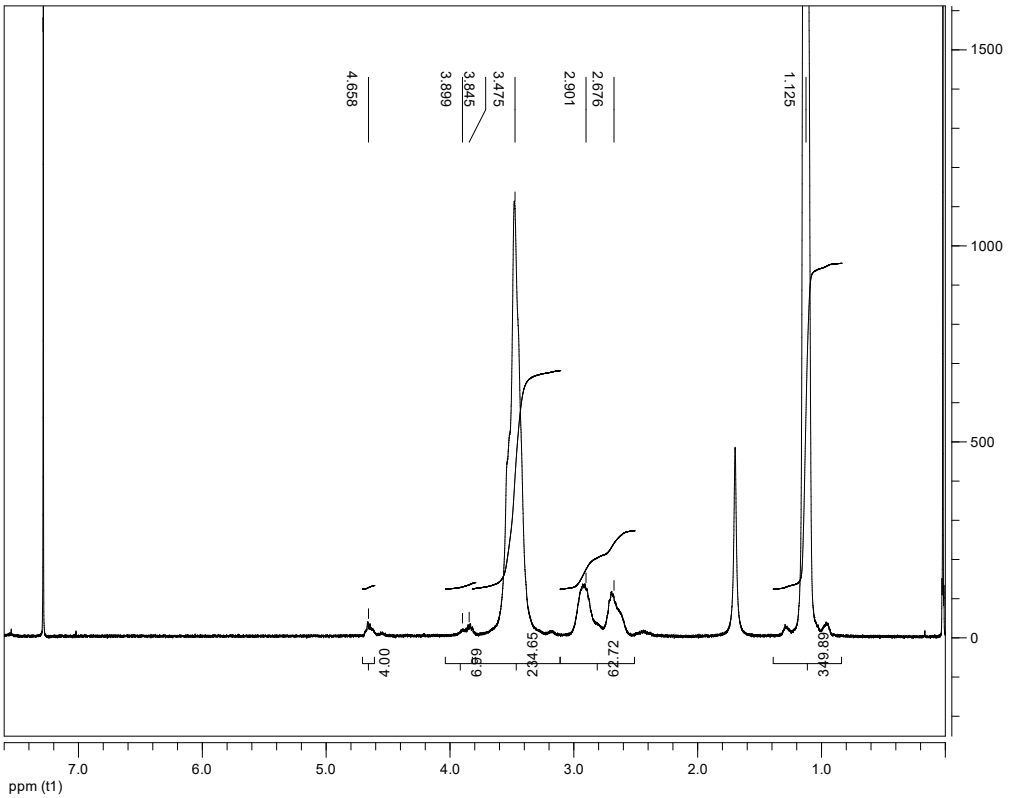

Fig.S3 FPIPOZ ^{1}H NMR spectrum in $CDCl_3$.

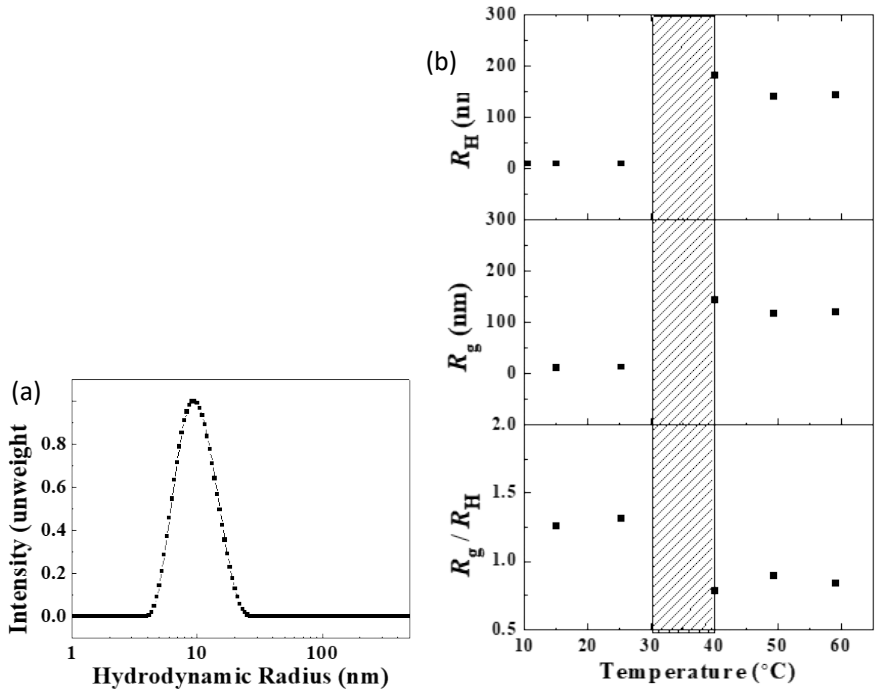

Fig.S4 (a) The hydrodynamic radius distribution of FPIPOZ aqueous solution with polymer concentration 1.0 g·L^{-1} at 20 °C by dynamic light scattering at a scattering angle of 90°. (b) The R_H, R_g and R_g/R_H of FPIPOZ aqueous solution as a function of temperature at 0.8 g·L^{-1}. The shaded area represents the temperature range where micrometer-sized aggregates could be found.

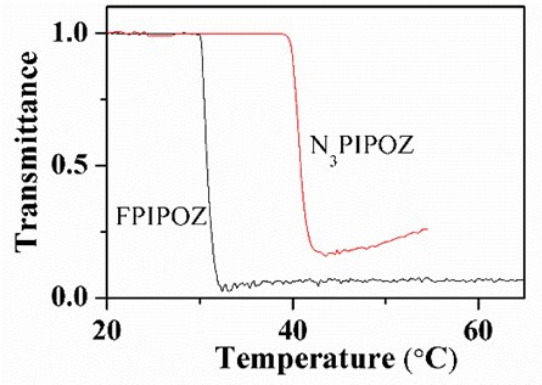

Fig. S5 Optical transmittance of the FPIPOZ and N_3PIPOZ aqueous solutions (polymer concentration 1.0 g·L^{-1}).

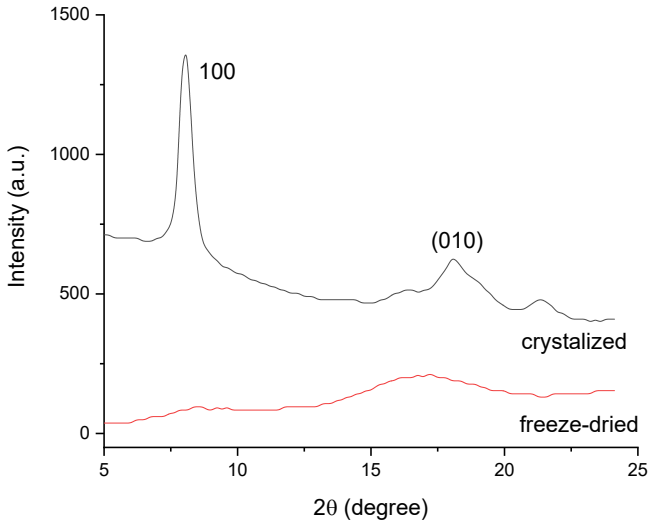

Fig.S6 XRD data of the freeze-dried FPIPOZ (red line) and that recovered from water after heating at 65 °C for 24 h (black line).

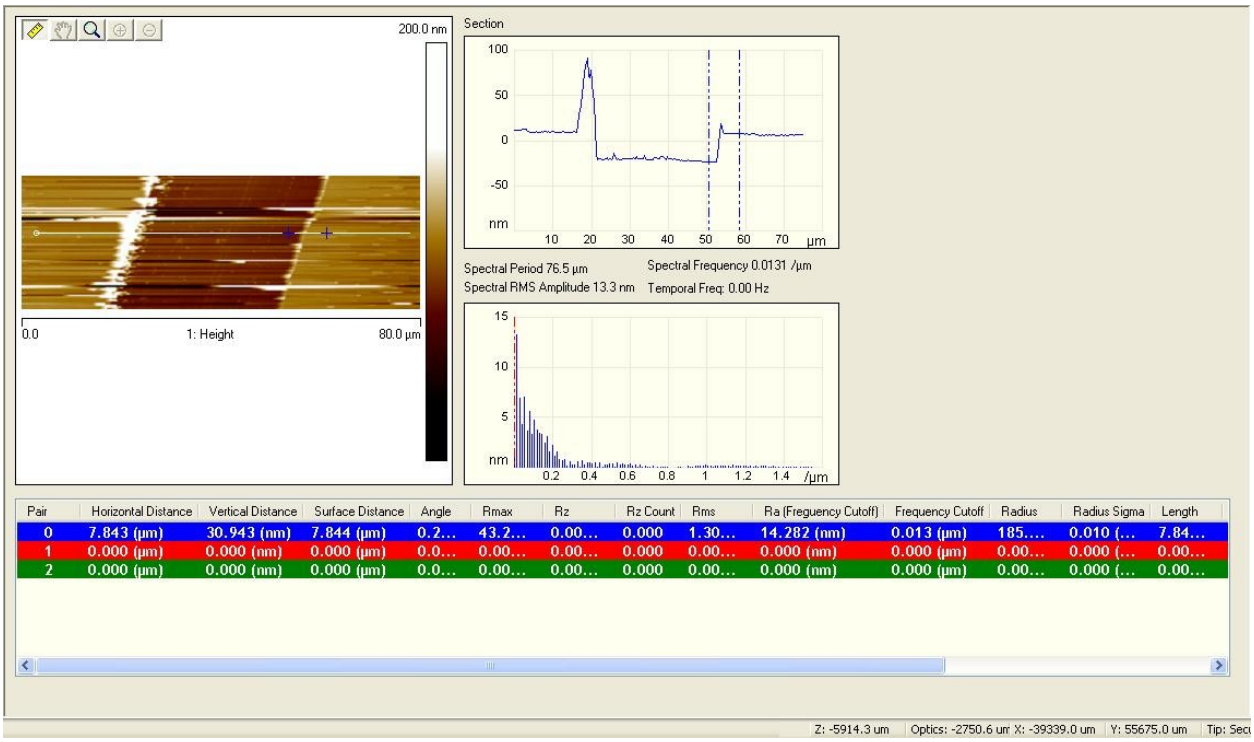

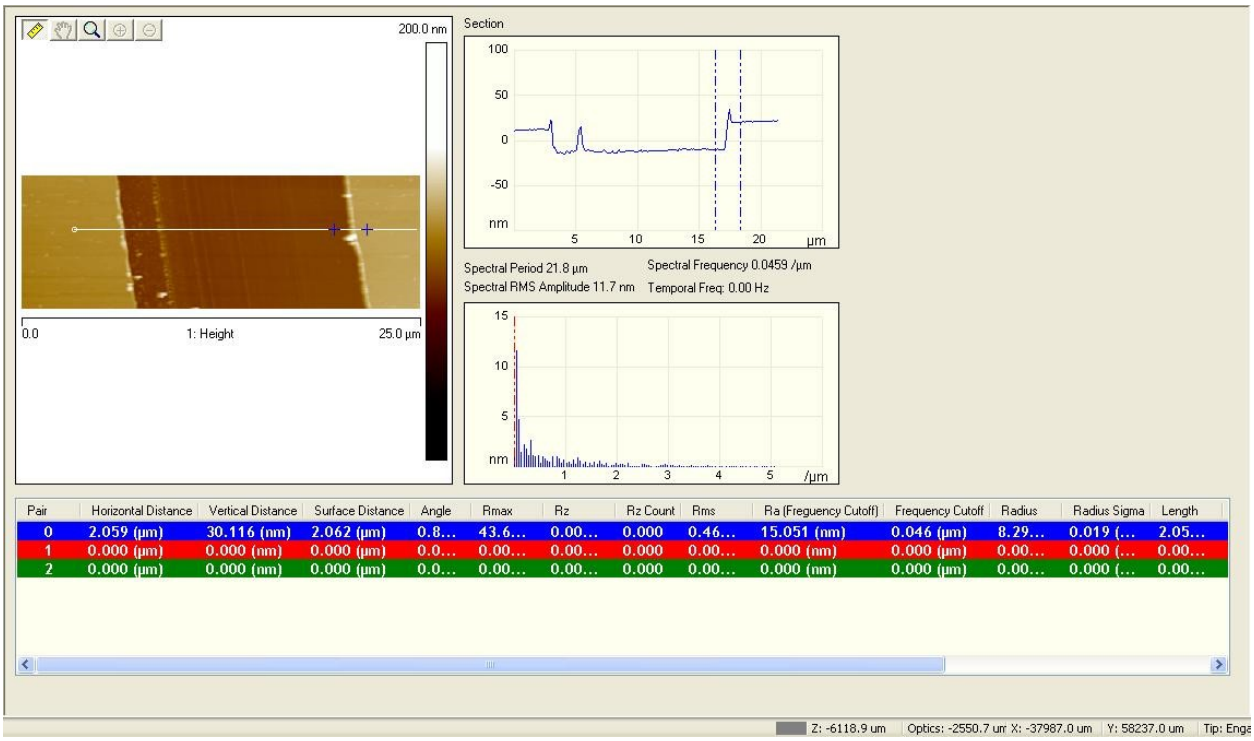

Fig. S7 Sections of scratched FPIPOZ (upper) and N_3PIPOZ (lower) films spin-coated from THF solutions with polymer concentration $5 g \cdot L^{-1}$.

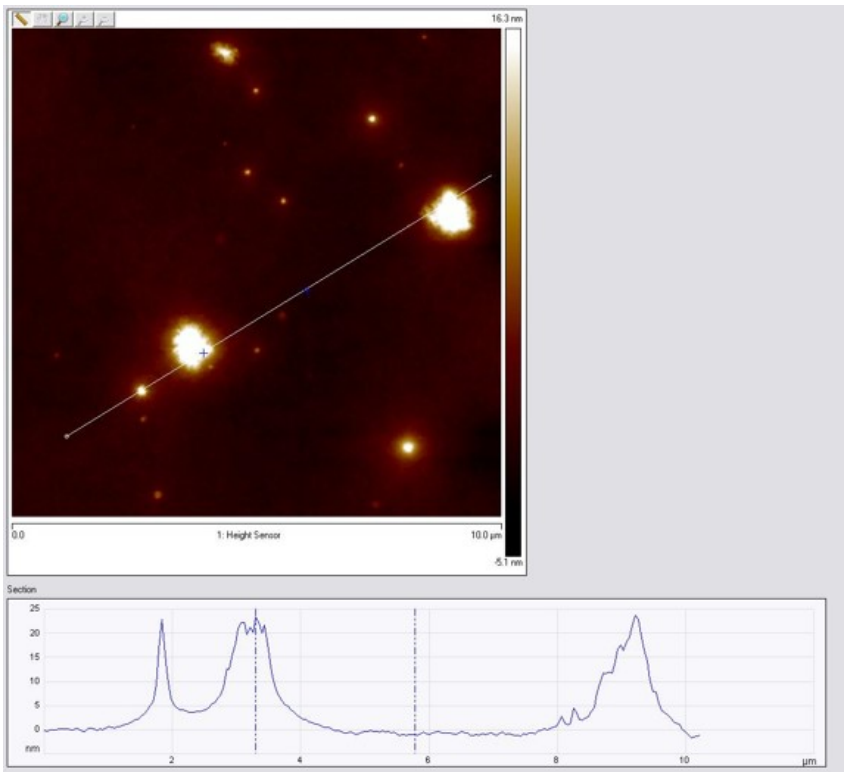

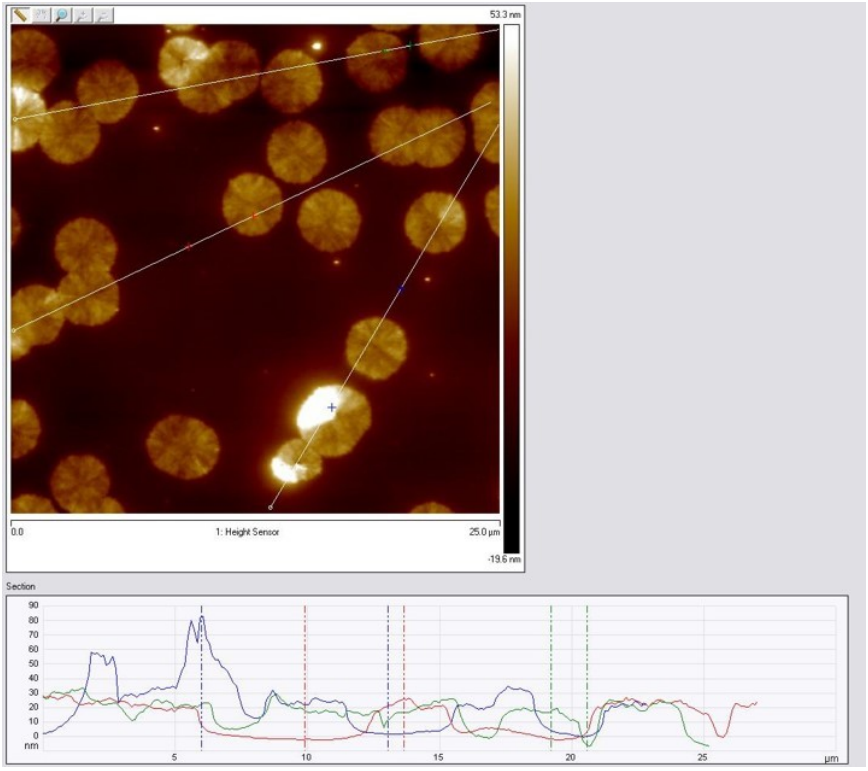

Fig. S8 Sections of N_3PIPOZ (upper) and FPIPOZ (lower) films after annealing in THF vapor at 70% saturation for 2 (top) and 7 hours (bottom) respectively at 22 °C.